Marion, D., Ikura, M., & Bax, A. (1989) *J. Magn. Reson. 84*, 425–428.
Marsh, D. G. (1975) in *The Antigens* (Sela, M., Ed.) Vol. III, pp 271–359, Academic Press, New York.
Marsh, D. G. (1986) *J. Allergy Clin. Immunol. 76* (Suppl.), 242–248.
Marsh, D. G., Hsu, S. H., Roebber, M., Kautzky, E. E., Freidhoff, L. R., Meyers, D. A., Pollard, M. K., & Bias, W. B. (1982) *J. Exp. Med. 155*, 1439–1451.
Marsh, D. G., Zwollo, P., Huang, S. K., Ghosh, B., & Ansari, A. A. (1990) *Cold Spring Harbor Symp. Quant. Biol. 54*, 459–470.
Mole, L. E., Goodfriend, L., Lapkoff, C. B., Kehoe, J. M., & Capra, J. D. (1975) *Biochemistry 14*, 1216–1220.
Mueller, L. (1987) *J. Magn. Reson. 72*, 191.
Mueller, L., & Ernst, R. R. (1979) *Mol. Phys. 38*, 963–992.
Nilges, M., Gronenborn, A. M., & Clore, G. M. (1988) *FEBS Lett. 239*, 129–136.
Otting, G., Widmer, H., Wanger, G., & Wuthrich, K. (1986) *J. Magn. Reson. 66*, 187–193.
Piantini, U., Sorensen, O. W., & Ernst, R. R. (1982) *J. Am. Chem. Soc. 104*, 6800–6801.
Rance, M., Sorensen, O. W., Bodenhausen, G., Wanger, G., Ernst, R. R., & Wuthrich, K. (1983) *Biochem. Biophys. Res. Commun. 69*, 979–987.
Richardson, J. S. (1981) *Adv. Protein Chem. 34*, 167–339.
Roebber, M., Klapper, D. G., Goodfriend, L., Bias, W. B., Hsu, S. H., & Marsh, D. G. (1985) *J. Immunol. 134*, 3062–3069.
Sette, A., Buus, S., Colon, S., Smith, J. A., Miles, C., & Grey, H. M. (1987) *Nature 1328*, 395–399.
Srinavasan, N., Sowdhamini, R., Ramakrisnan, C., & Balaram, P. (1990) *Int. J. Pept. Protein Res. 36*, 147–155.
States, D. J., Haberkorn, R. A., & Ruben, D. J. (1982) *J. Magn. Reson. 48*, 286–292.
Unanue, E. R., & Allen, P. M. (1987) *Science 236*, 551–557.
Vidusek, D. A., Roberts, M. F., & Goodfriend, L. (1985) *Biochemistry 24*, 2747.
Wuthrich, K. (1986) *NMR of Proteins and Nucleic Acids*, Wiley-Interscience, New York.
Zwollo, P., Ehrlich-Kautzky, E., Ansari, A. A., Scharf, S. J., Erlich, H. A., & Marsh, D. G. (1991) *Immunogenetics 33*, 141–151.

Kinetics and Mechanism of the Folding of Cytochrome *c*†

Kenneth M. Pryse,[‡,§] Thomas G. Bruckman,[§,∥] Bruce W. Maxfield,[⊥,#] and Elliot L. Elson*[,‡,§]
Department of Biochemistry and Molecular Biophysics, Washington University School of Medicine, St. Louis, Missouri 63110, and Departments of Chemistry and Physics, Cornell University, Ithaca, New York 14853
Received January 7, 1992; Revised Manuscript Received March 25, 1992

ABSTRACT: The reversible folding of cytochrome *c* in urea at pH 4.0 was investigated by repetitive pressure perturbation kinetics and by equilibrium spectroscopic methods. Two folding reactions were observed in the 1 ms to 10 s time range. The rates and amplitudes of these reactions depend on urea concentration in a complex manner, which is different for each process. The absorbance spectra of the kinetic amplitudes of the two reactions also differ from each other. A model with a three-state mechanism can quantitatively account for all of the kinetic and equilibrium data, and it enables us to determine the rate constants and volume changes of the two steps. If a rapid protonation step is added to the mechanism, the analysis can be extended to calculate the pH dependence of the rate and amplitude of the faster folding step. This pH dependence is in excellent agreement with previously published data [Tsong, T. Y. (1977) *J. Biol. Chem. 252*, 8778–8780]. Kinetic experiments in the 695-nm band show clearly that the axial ligand methionine-80 is involved in the slow folding process and the other axial ligand, histidine-18, is involved in the fast process. Additional experiments with a cyanogen bromide fragment of the protein, and fluorescence detection of the folding kinetics of the intact protein, support an interpretation of the model in terms of known structural elements of cytochrome *c*. This work provides new information about the mechanism of the folding of cytochrome *c*, resolves conflicts in earlier interpretations, and demonstrates the applicability of the repetitive pressure perturbation kinetics method to protein folding.

The role of hydrophobic interactions in stabilizing the folded conformations of proteins is a long-standing problem of protein physical chemistry (Kauzmann, 1959; Privalov & Gill, 1988). The thermodynamic properties of these interactions are not yet well understood. Although solvent transfer experiments provide a useful model for the heat capacity changes associated with protein folding [e.g., Baldwin (1986)], they are less successful in accounting for the corresponding volume and compressibility changes [e.g., Kauzmann (1987)]. Nevertheless, the response of the protein conformation to changes in pressure, which is governed by the differences among the volumes of the conformational states, can usefully complement measurements of the response of the protein to temperature changes, which is governed by differences in enthalpy. Both enthalpy and volume changes are thought to be dominated by changes in interactions of water molecules with each other due to the exposure of amino acids to the solvent during unfolding (Edsall & McKenzie, 1983).

† This work was supported by grants from NIH (GM-38838) and the Lucille P. Markey Charitable Trust to E.L.E.
* Author to whom correspondence should be addressed at Department of Biochemistry and Molecular Biophysics, Box 8231, Washington University School of Medicine, 660 S. Euclid Ave., St. Louis, MO 63110.
‡ Department of Biochemistry and Molecular Biophysics, Washington University.
§ Department of Chemistry, Cornell University.
∥ Current address: Betz Laboratories, Inc., Somerton Rd., Trevose, PA 19047.
⊥ Department of Physics, Cornell University.
Current address: Industrial Sensors, 400 Hester St., San Leandro, CA 94577.

0006-2960/92/0431-5127$03.00/0

One approach, which has been little used, is to decompose the net volume change for protein folding into the volume changes for the separate time-resolved components associated with the different kinetic phases of the process. Then, if structural information about the different components is available, this could be used to interpret the origins of the partial volume changes. Conversely, once volume changes are better understood, they could be used to help interpret kinetic mechanisms in structural terms. In this paper, we illustrate this approach in a study of the kinetics of the folding of cytochrome *c* using the method of repetitive pressure perturbation kinetics (RPPK)[1] (Clegg et al., 1975; Clegg & Maxfield, 1976).

The RPPK method measures the pressure-induced relaxation kinetics of reaction systems in liquid solution. The reaction system is subjected to a small (15 bar) rapid change in pressure, and then the progress of the reaction to the new equilibrium state is monitored optically, e.g., by absorbance, fluorescence, or light scattering. Although the response of a typical system to a single pressure jump of this size is ordinarily buried in noise, signal averaging of repeated jumps provides good accuracy and allows the method to be used even on systems with relatively small volume changes. Although potentially useful in a wide range of studies, the method has been little used since its introduction. Halvorson, however, has studied the self-association of glutamate dehydrogenase with RPPK (Halvorson, 1979), and the method has recently been applied to the interaction of ethidium bromide with DNA (Macgregor et al., 1985; Macgregor & Clegg, 1987).

The folding of cytochrome *c* has often been studied to determine both the forces which stabilize its folded conformation and the sequence of events which occur when the protein unfolds or refolds. Most experiments have been conducted at neutral pH in the presence of denaturants such as urea and GuHCl or in highly acidic solutions of pH 2.0 or lower. The kinetics of folding has previously been studied by rapidly changing the solvent composition or temperature. In an RPPK measurement, the small pressure change causes only a very small conformational free energy change. If the equilibrium state of the protein is far from the unfolding region, the pressure jump is too small to cause a measurable conformational change. Hence, it is necessary to carry out the measurements on partially unfolded molecules. In these experiments, the protein is held at an acidic pH and placed at various extents of folding by varying the urea concentration. The folding pathway for cytochrome *c* under these conditions is not yet well established. Hence, the main purposes of this first paper are to measure the kinetics, to develop a minimal mechanism, and to provide a structural interpretation of the mechanism. We have observed two kinetic components of the folding process, characterized their rates, amplitudes, and spectroscopic properties, quantitatively fitted the data to a simple but detailed model, and proposed a structural interpretation of the results. The kinetic and equilibrium data indicate differences in the conformational processes which occur in the two component reactions and suggest some structural properties of the intermediate state.

Materials and Methods

Horse heart ferricytochrome *c*, type VI, was purchased from Sigma Chemical Co. This type is over 95% pure, and since further purification did not change the folding kinetics the protein was usually used without additional purification. Urea was ultrahigh purity from Schwarz-Mann. All urea solutions were used within 24 h of preparation. A fragment of cytochrome *c*, obtained by cleaving the protein with cyanogen bromide, was generously provided by Dr. Richard P. Junghans. Other reagents were of analytical grade.

The repetitive pressure perturbation apparatus has been described in detail elsewhere (Clegg & Maxfield, 1976). Briefly, about 0.7 mL of solution is contained in a cylindrical synthetic sapphire cell. Thin diaphragms isolate the solution from a piezoelectric crystal stack at one end of the cell which compresses the solution and from a pressure transducer at the other end which reads out the applied pressure. The crystal stack is driven by a square-wave voltage change, producing a repetitive, rectangular pressure pulse. The light from a mercury arc lamp or tungsten filament lamp is passed through a monochromator and focused on the cell. A photomultiplier detects either the transmitted light or the fluorescence of the sample. The photomultiplier current is compared to a reference signal by a ratio circuit, digitized, and averaged over many on–off pressure cycles until the desired signal to noise ratio is reached. The data are then transferred directly to a computer for analysis.

Some improvements have been made to the original apparatus. An Oriel lamp housing (Model 6140) with a two-element f/1.0 UV grade fused silica condensing lens provides a higher light intensity at the sample. A Schoeffel monochromator (Model 250 GM) is now used with either of two gratings: one blazed at 280 nm with a bandwidth of 1.7 nm/mm of slit width and one blazed at 350 nm with a bandwidth of 3.4 nm/mm. The experiments described here were done with a wavelength resolution of 2 nm or less. The reference and signal detectors were EMI 9558QF photomultipliers with quartz windows, selected for low drift. The differential amplifier used to decrease intensity fluctuations from arc jumps has been replaced by a ratio circuit resulting in greater stability and improved signal to noise. Changes in crystal stack construction have increased the pressure change to about 10–15 bar. These and other improvements in optical alignment and calibration of the instrument are described in more detail elsewhere (Bruckman, 1977).

The kinetic data were fit with an exponential function, $\Delta A \exp(-t/\tau)$, by a combination of linearization of the fitting function and the method of gradient search (Bevington, 1969). The kinetic amplitude of the relaxation curve, ΔA, was converted from signal averager units to absorbance by calibration of the signal averager input and determination of the effective path length of the sample cell. Division by the total number of pressure jumps and the pressure change per jump gives the reported values of the kinetic amplitudes in absorbance per bar.

The compression produced by the volume change is essentially adiabatic and therefore produces a temperature change in the solution given by $\Delta T = TV\alpha\Delta P/C_p$ where V is the molar volume, $\alpha = (\partial V/\partial T)_p(1/V)$, and C_p is the molar heat capacity. For water at 20 °C, a pressure increase of 15 bar produces a temperature change of $\approx 2.3 \times 10^{-2}$ °C. The effect of this temperature increase on the equilibrium constant depends on the magnitude of the molar enthalpy change, ΔH. The temperature of the pressure perturbation experiments, 20 °C, is very close to the temperature where the enthalpy of folding of cytochrome *c* is zero (Privalov, 1979). The enthalpy change under our experimental conditions is about 2 kcal/mol. The resulting change in the equilibrium constant is given by

$$\Delta K/K \approx \ln (K_f/K_i) = (\Delta H^\circ/R)(\Delta T/T^2) = 2.6 \times 10^{-4}$$

[1] Abbreviations: RPPK, repetitive pressure perturbation kinetics; GuHCl, guanidine hydrochloride.

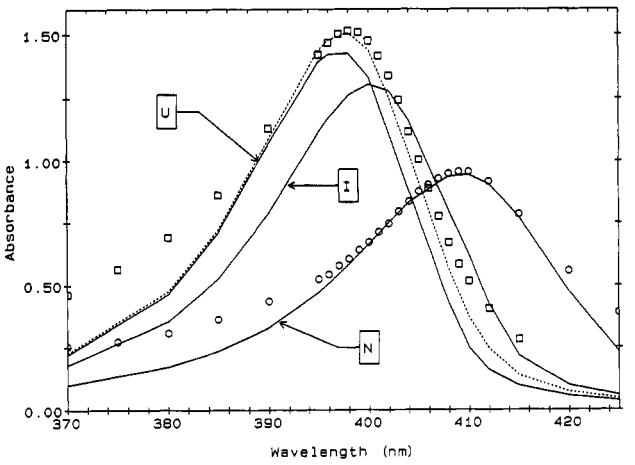

FIGURE 1: Absorbance spectra of cytochrome *c* in 0 M urea (○) and 8.0 M urea (□), pH 4.0. Solid lines are theoretical spectra of the N, I, and U forms of the protein, calculated with the parameters in Table II. The spectrum of the U form is for 0 M urea. The dashed line is the calculated spectrum at 8.0 M urea composed of an equilibrium mixture of the I and U spectra. The ratio of [U]/[I] is determined by the parameters in Table I.

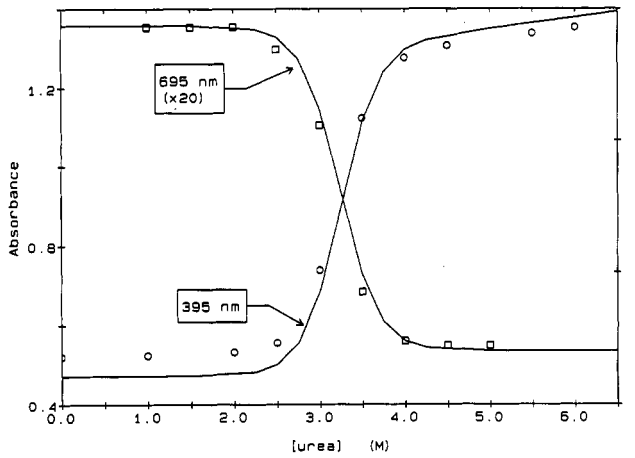

FIGURE 2: Absorbance of cytochrome *c* as a function of urea concentration at 395 nm (○) and 695 nm (□). Solid lines are calculated from the model described in the text and the parameters in Table II.

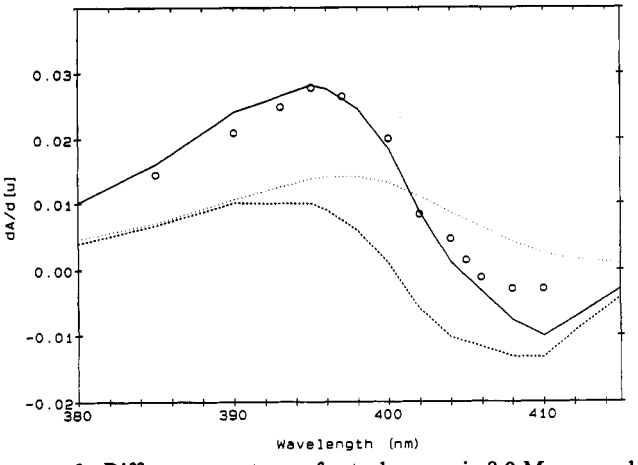

FIGURE 3: Difference spectrum of cytochrome *c* in 8.0 M urea and 5.0 M urea. The solid line is calculated from the model with both K_1 and ϵ_U dependent on urea; the dashed line is from that with K_1 dependent on urea and ϵ_U constant; the dotted line is from that with ϵ_U dependent on urea and K_1 constant.

For a volume change of −30 mL/mol, the change in the equilibrium constant due to the pressure increase is

$$\Delta K/K \approx \ln (K_f/K_i) = -\Delta V^\circ \Delta P/RT = 1.9 \times 10^{-2}$$

which is over 70-fold greater than that due to the temperature increase.

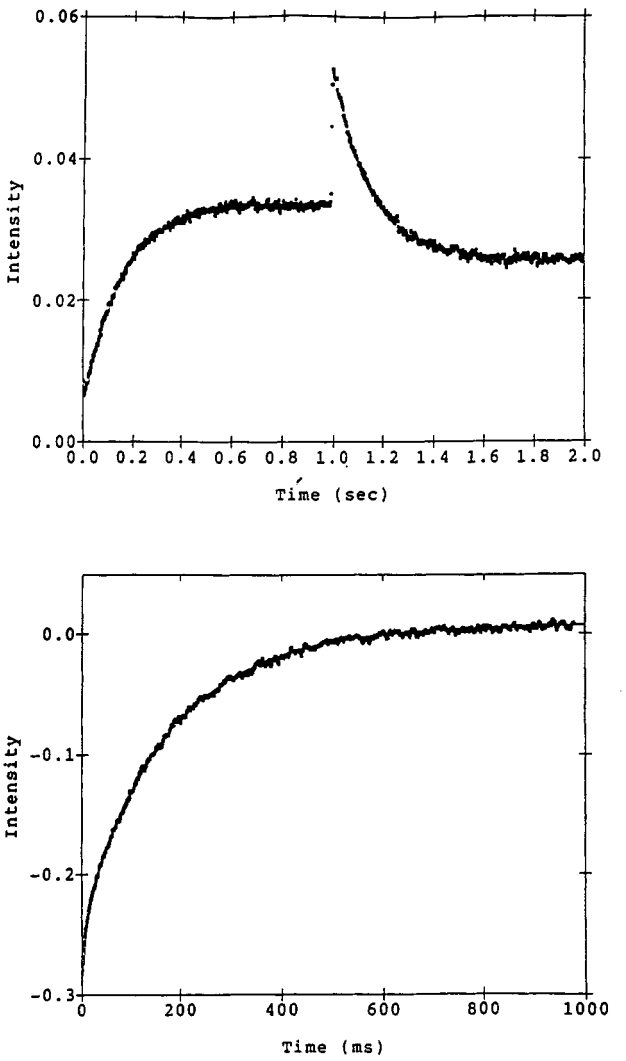

FIGURE 4: Cytochrome *c* folding data with least-squares fits superimposed. Solution conditions: 5.0 mg/mL cytochrome *c*, pH 4.0, 3.5 M urea, 0.020 M acetate buffer, 0.010 M Cl^-. Pressure change: 15.3 bar. (top) Complete on–off pressure cycle. Each half of the cycle was fit by a single exponential. Wavelength: 700 nm. Amp_{on} = 0.0276, τ_{on} = 153 ms, Amp_{off} = 0.0278, τ_{off} = 156 ms. (bottom) The pressure on and pressure off halves are combined. The data were fit by a double exponential. Wavelength: 550 nm. Amp_1 = −0.0528, τ_1 = 11.9 ms, Amp_2 = −0.248, τ_2 = 175 ms.

RESULTS

Equilibrium Spectra. The absorbance of the Soret band of cytochrome *c* in 0 M and 8.0 M urea, pH 4.0, are given in Figure 1. The blue shift and more intense absorbance at higher urea concentrations indicate the conversion of the iron from low spin to high spin. Addition of urea causes a sharp increase in the absorbance of the Soret band at 395 nm and a sharp decrease of the 695-nm band (Figure 2), which has been shown to be sensitive to Met-80 liganding (Sreenathan & Taylor, 1971) as well as to the conformation of the polypeptide chain (Myer, 1980). This transition is centered at 3.3 M urea, but after it is complete at ≈4.0 M urea the 395-nm absorbance continues to increase gradually. The difference spectrum for this posttransition increase is shown in Figure 3. In contrast, the change in the 695-nm absorbance is complete at ≈4.0 M urea. The fluorescence of the single tryptophan residue, Trp-59, has the same urea dependence as the Soret absorbance (Bruckman, 1977).

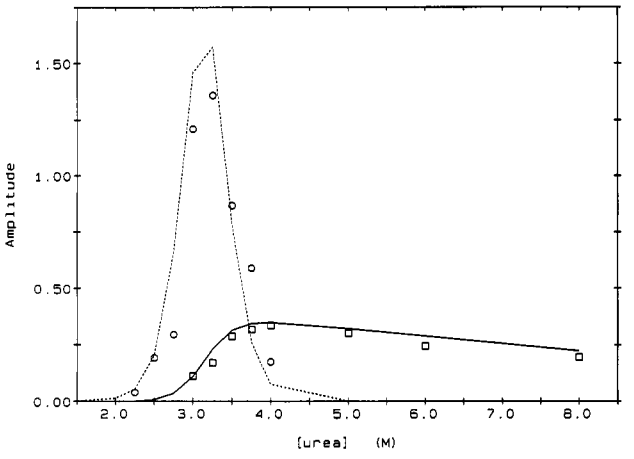

FIGURE 5: Kinetic amplitudes of the fast (□) and slow (○) processes as a function of urea concentration. ΔA^{01} was measured at 404 nm and ΔA^{02} was measured at 400 nm. ΔA^{01} is inverted in sign in this graph. The dashed and solid lines are calculated from the model at the respective wavelengths.

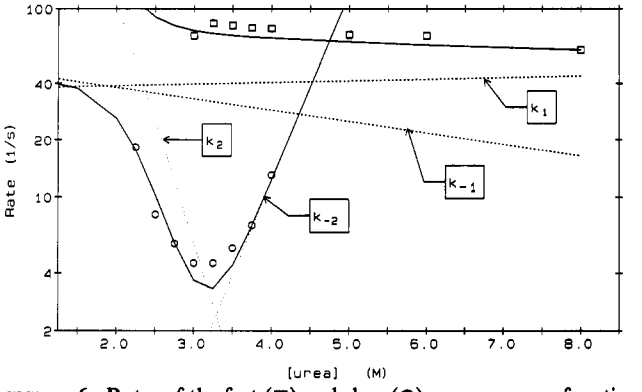

FIGURE 6: Rates of the fast (□) and slow (○) processes as a function of urea. The solid lines are calculated from eqs 3a and 3b and the parameters in Table I. The dashed and dotted lines show the calculated urea dependence of the underlying rate constants.

Kinetics of Folding. Two processes were observed in presence perturbation kinetic experiments in the time range from 1 ms to several seconds. Figure 4 illustrates the quality of the data and also shows computer-determined best fits to the data. The kinetic amplitudes as a function of urea concentration are shown in Figure 5. The faster reaction was present at all urea concentrations above 2.5 M, indicating that some kind of structural change affecting the heme takes place even in very concentrated urea solutions. The slower process, however, could be seen only within the major transition, approximately 2.5 M to 4.5 M urea. The amplitude maximum of the slower reaction coincides with the center of the sharp equilibrium transition, while the faster reaction reaches its maximum amplitude near the end of the major equilibrium transition.

The rates of the two processes differ in their dependence on denaturant concentration (Figure 6). The rate of the slower step decreases sharply with increasing urea concentration and then increases rapidly, the minimum in rate occurring when the amplitude is at its maximum. The faster step becomes gradually slower over the full range of denaturant concentration.

The kinetic amplitudes as a function of wavelength are shown in Figure 7. The amplitude spectrum of the slower relaxation is congruent with the equilibrium difference spectrum. The maximum, minimum, and isosbestic point of the faster relaxation are about 4 nm higher than those of the slower step. This spectral difference was helpful not only in interpretation of the model, but also for experimentation, since each process could be observed without interference from the other by selecting the appropriate wavelength.

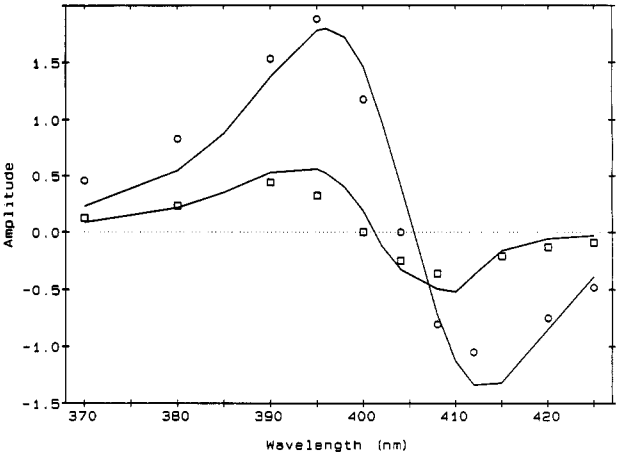

FIGURE 7: Kinetic amplitudes of the fast (□) and slow (○) reactions as a function of wavelength. ΔA^{01}, the fast step, was measured at 5.0 M urea and ΔA^{02} was measured at 3.25 M urea. Solid lines are calculated from the model at the respective denaturant concentrations.

To help establish the roles of the axial ligands in the two kinetic processes, we performed pressure perturbation experiments on concentrated protein samples using wavelengths in the 540-nm and 695-nm absorbance bands, since the 695-nm band is a sensitive indicator of the presence of the Met-80 axial ligand. Data at two representative wavelengths are shown in Figure 4 for a solution of cytochrome *c* at 5.0 mg/mL, 3.5 M urea, pH 4.0. At all wavelengths in the 695-nm band, the data were fit very closely by a single exponential with a time constant of 155 ms, while in the 540-nm band, two exponentials with time constants of 160–170 ms and 10–14 ms were required to fit the data. We were also able to see both processes with similar time constants on the edge of the Soret band at 450–460 nm with this same sample. Closer to the center of the Soret region, the absorbance was too great to record any signal. Similar results were obtained at 3.0 M urea. At 5.0 M urea, pH 4.0, no kinetic signal could be seen in the 695-nm band, and only a 13-ms process was observed in the 540-nm region and at the edge of the Soret band.

Kinetic experiments were done at several urea concentrations in which the tryptophan-59 fluorescence was monitored (Bruckman, 1977). Unlike the absorbance measurements, only a single relaxation was seen at all urea concentrations. The time constants and the dependence of the amplitudes on urea were the same as those of the slower process seen via absorbance. The minimum in rate coincided with the maximum in amplitude. No relaxation time in the 2 ms–20 ms range was seen, although calculations based on the model described in the next section indicate that the faster process should be visible using fluorescence detection (Pryse, 1988). Other workers have been able to detect both modes using fluorescence, although under different experimental conditions from ours (Roder et al., 1988). Our failure to detect it is probably due to the very low light levels produced.

Another set of experiments used a protein fragment, produced by cleavage of the protein at methionine residues with cyanogen bromide, which contains residues 1–64 of the polypeptide chain. This fragment has the normal covalent attachments to the heme at residues 13 and 17. The fluorescence of this fragment is high at all urea concentrations at pH 4.0, indicating that it does not have a compact conformation similar to that of the native protein. Pressure perturbation absorbance measurements with fragment 1–64 showed a process which

is similar to the faster step observed with the intact protein. Its relaxation time was in the 10–15-ms range, and the isosbestic wavelength of the amplitude was 400 nm. The relaxations of the derivative were observed at lower urea concentrations than were those of the intact protein, however, suggesting that any structural elements that are present in the fragment are more susceptible to disruption by urea than are similar elements in the intact protein. No other relaxations were observed on longer time scales.

Model. The kinetic and equilibrium data are consistent with a simple three-state mechanism of folding:

$$U \underset{k_1}{\overset{k_{-1}}{\rightleftharpoons}} I \underset{k_{-2}}{\overset{k_2}{\rightleftharpoons}} N$$

where

$$K_1 = k_1/k_{-1} = [U]/[I] \tag{1a}$$

and

$$K_2 = k_2/k_{-2} = [N]/[I] \tag{1b}$$

N, I, and U represent the native, intermediate, and unfolded forms of the protein. The I $\rightleftharpoons$ U reaction is designated reaction 1, because it is taken to be the faster step under our experimental conditions. [Throughout this paper, we refer to the two reactions which we see as the "fast" and "slow" steps, even though reaction 2 (the slow step) depends on urea much more strongly than reaction 1 so that outside the transition region it is actually faster than reaction 1. In an equilibrium perturbation kinetics experiment outside the transition region, however, the amplitude of the slow step is below the limits of detection.] k_1 and k_{-1} are assigned to the "reverse" and "forward" reactions, respectively, since this leads to more symmetrical mathematical expressions for the relaxation times and amplitudes.

An equation for any experimentally measured equilibrium property, S, as a function of urea concentration can be derived from simple mass-action considerations:

$$S = C_0(\sigma_N K_2 + \sigma_I + \sigma_U K_1)/(1 + K_1 + K_2) \tag{2}$$

where C_0 is the total concentration of protein, σ_X is the appropriate coefficient of species X for the property being measured, and the K_i's are dependent on urea as defined below. To calculate the absorbance as a function of urea concentration, molar extinction coefficients for the three species would be used in place of the σ_X.

Equations for the rates and kinetic amplitudes are given by the general theory of chemical relaxation for multistep reactions (Eigen & DeMayer, 1963). Generally, the reaction steps are coupled such that each relaxation time does not correspond to a single reaction step but instead has contributions to varying degrees from the rate constants of several steps. Simplification of the most general equations is possible when the time constants of the two processes differ by a fact of 10 or more. Then, the faster step reaches its new equilibrium before the slow step has progressed appreciably, and the faster step can be treated independently. In deriving the equations for the slow step, it is assumed that the fast process is at equilibrium. In practice, the general equations for the coupled case were used throughout our analysis. The approximate uncoupled equations are presented here, however, since they are applicable to most of the experiments analyzed, and they show more clearly the relationship between the relaxation times and the individual processes.

The expressions for the relaxation times are the following:

$$(\tau_1)^{-1} = k_1 + k_{-1} \tag{3a}$$

$$(\tau_2)^{-1} = k_{-2} + k_2/(1 + K_1) \tag{3b}$$

The concentration changes for the faster step are given by

$$\Delta C_U^{01} = -\Delta C_I^{01} = C_0 \frac{K_1}{(1 + K_1)(1 + K_1 + K_2)} \frac{\Delta K_1}{K_1} \tag{4a}$$

and

$$\Delta C_N^{01} = 0 \tag{4b}$$

where $C_0 = C_N + C_I + C_U$. The superscripts 01 and 02 refer to the fast and slow steps. Equation 4b is a consequence of assuming that the reaction N $\rightleftharpoons$ I is much slower than the reaction I $\rightleftharpoons$ U.

For the slow step

$$\Delta C_U^{02} = K_1 \Delta C_I^{02} = -K_1/[1 + K_1]\Delta C_N^{02} = C_0 \left[\frac{K_1 K_2}{(1 + K_1)(1 + K_1 + K_2)}\right] \times \left[\frac{\Delta K_2}{K_2} - \frac{K_1}{1 + K_1}\frac{\Delta K_1}{K_1}\right] \tag{5}$$

where $\Delta K_i/K_i = -\Delta V_i^0 \Delta P/RT$, for $\Delta K_i/K_i \ll 1.0$. ΔV_i^0 is the molar volume change of the ith reaction step, ΔP is the applied pressure change, R is the gas constant, and T is the temperature in Kelvin.

The experimentally measured kinetic amplitude, however, is the change in absorbance, ΔA, which depends on the concentration changes and the molar extinction coefficients, ϵ_X. For the faster step

$$\Delta A^{01} = \epsilon_I \Delta C_I^{01} + \epsilon_U \Delta C_U^{01} = [\epsilon_I - \epsilon_U]\Delta C_I^{01} \tag{6}$$

and for the slower step

$$\Delta A^{02} = \epsilon_N \Delta C_N^{02} + \epsilon_I \Delta C_I^{02} + \epsilon_U \Delta C_U^{02} = [-\epsilon_N[1 + K_1]/K_1 + \epsilon_I/K_1 + \epsilon_U]\Delta C_U^{02} \tag{7}$$

Some of the parameters in these equations must depend on urea concentration to account for the variation of the measured properties. We suppose that the logarithm of each microscopic rate constant depends linearly on denaturant concentration:

$$\ln k_i = m_i + n_i[\text{urea}] = \ln k_i^0 + n_i[\text{urea}] \tag{8}$$

This simple functional dependence has been used previously (Ikai et al., 1973) and leads directly to the same dependence on denaturant concentration for the equilibrium constants:

$$\ln K_i = (m_i - m_{-i}) + (n_i - n_{-i})[\text{urea}] = \ln K_i^0 + \Delta n_i[\text{urea}] \tag{9}$$

This is equivalent to the statement that the differences in free energy between N and I and between I and U depend linearly on denaturant concentration and is often used in equilibrium folding studies.

The absorbance spectrum of the protein does not vary below 2.5 M urea, and so we take ϵ_N to be independent of urea. Although the kinetic data can be fit reasonably well with constant values for ϵ_I and ϵ_U, the equilibrium difference spectrum shown in Figure 3 requires that at least one of them vary with urea concentration. This posttransition change in absorbance from 4.5 M to 8.0 M urea could be due to one or both of two factors: (1) the changing equilibrium constant K_1, producing a shift from the spectrum of I to that of U; (2) a change in ϵ_I or ϵ_U (or both), produced by the change in solvent conditions. If $\partial A/\partial[u]$ (the change in absorbance with urea concentration) were due only to a change in the relative concentrations of I and U, then a plot of $\partial A/\partial[u]$ vs wave-

length would have the shape of the difference spectrum of I and U. If $\partial A/\partial[u]$ were due only to an increase in ϵ_I of ϵ_U or both, then the $\partial A/\partial[u]$ spectrum would have the shape of an absorbance spectrum. The experimental $\partial A/\partial[u]$ spectrum cannot be approximated by either shape alone, but it appears to be a composite of both. We have taken ϵ_U to depend on urea concentration in the following manner:

$$\epsilon_U = \epsilon_U^0(1 + \partial\epsilon/\partial[u]) \quad (10)$$

Alternatively, we could have taken ϵ_I to be the urea-dependent extinction coefficient. However, I is present in smaller amounts than U, and it would take an unreasonably large increase in ϵ_I to account for the observed increase in absorbance. Also, U is considered the most unfolded species and therefore its heme chromophore is the most exposed to solvent.

The absorbance, A, of the three species can be calculated with the equation (Champion & Albrecht, 1979)

$$A = C\left(\left\{\frac{\delta\Theta_e}{\Pi - \Theta_+} + \Gamma\right\}(\Delta_e + \epsilon_0)^2 + \left\{\frac{\delta\Theta_e}{\Pi - \Theta_+} - \Gamma\right\} \times (\delta^2 - \Gamma^2) + \frac{\Gamma\delta(\Delta_e + \epsilon_0)}{\Pi - \Theta_+} \ln\left\{\frac{\epsilon_0^2 + \delta^2}{\Delta_e^2 + \Gamma^2}\right\}\right) \Big/ ([(\Delta_e + \epsilon_0)^2 + (\Gamma + \delta)^2][(\Delta_e + \epsilon_0)^2 + (\Gamma - \delta)^2]) \quad (11)$$

where $\Delta_e = E_{e0} - hc/\lambda$, $\Theta_+ = \tan^{-1}(\delta/\epsilon_0)$, $\Theta_e = \Pi - \tan^{-1}(\Gamma/\Delta_e)$, and E_{e0} is the energy of the transition, which determines the position of the peak; Γ is the homogeneous broadening constant and is one of the primary determinants of the width of the band; δ and ϵ_0 are the width and centroid of the truncated Lorentzian representing the product of the Franck–Condon factors with the density of states function and together determine the asymmetry; C is an intensity scaling factor; h is Planck's constant; c is the speed of light; and λ is the wavelength of incident light. Since the porphyrin chromophore is distorted in the x–y plane, there will be two such terms for each absorption band, differing in E_{e0} by the splitting energy, Δ_{xy}. Two of these variables, ϵ_0 and the x–y splitting, can be estimated from other independent spectroscopic experiments, as discussed by Champion and Albrecht, and we have used their values for these parameters. The transition energy for the native state can be obtained directly from the wavelength maximum of the spectrum in low urea, and we require the transition energy of the intermediate to be between those of the N and U forms. Estimates of the broadening constants Γ and δ can also be obtained from the widths and asymmetric nature of the experimental spectra, and we again require the values for the intermediate to be close to or between the values for the native and denatured forms.

Equations 1–11 provide a theoretical basis for the complete description of all the data presented in Figures 1–7. There are many parameters, but there are many constraints on the parameters due to the large amount of data and the different types of data encompassed by the model. Determination of the best values for all the parameters is a complex task, however, since each equation contains several parameters, and all of the parameters except one (ΔV^{02}) contribute to more than one of the measured properties. For instance, the slopes (m_2 and m_{-2}) and intercepts (n_2 and n_{-2}) of the rate constants k_2 and k_{-2} determine directly the calculated values of the slower rate as a function of urea. The same four parameters also go into the calculation of the kinetic amplitude ΔA^{02} and the equilibrium absorbance. In these cases, however, it is only the differences Δn and Δm which enter into the calculation, and several other parameters are also involved. Standard curve-fitting routines determine the best fit of a single function to a single experimental curve and thus are not adequate by themselves to handle models of this complexity. In our model, the set of parameter values which is best for one experimental curve, such as τ_2^{-1} vs [urea], is not necessarily the best set for a different curve, such as A_{395} vs [urea]. We therefore used a global modeling procedure which started with computer curve-fitting routines to determine values for a few parameters. These initial values were then used in conjunction with estimates for other parameters to calculate a wider range of experimental data. The parameter values were then systematically varied to achieve acceptable fits to all of the curves, determined by visual inspection. This procedure is described in more detail elsewhere (Pryse, 1988). The final set of parameter values used in calculating the curves shown in Figures 1–7 are given in Tables I and II.

Table I: Kinetic Parameters of the Model[a]

rate constants	k_1	k_{-1}	k_2	k_{-2}
n (intercept)	3.62	3.92	10.6	−6.7
m (slope)	0.02	−0.14	−2.95	2.3

[a] These parameters determine the value of the rate and equilibrium constants at any urea concentration using eqs 8 and 9.

Table II: Spectroscopic Parameters of the Model

protein species	N	I	U
relative intensity	330	405	420
δ, Lorentzian width (cm^{-1})	590	614	615
Γ, broadening constant (cm^{-1})	285	180	150
ϵ_0, centroid (cm^{-1})	400	400	400
excitation maximum (cm^{-1})	23 735	24 290	24 530
Δ_{xy}, x–y splitting (cm^{-1})	380	400	360
relative viscosity	3.5	18.0	26.0
absorbance (695 nm)	0.0575	0.008	0.008
$\partial\epsilon/\partial[u]$	0	0	0.015

It is difficult to gauge the precision with which the parameters of the model are determined due to the complexity and scope of the model itself. We have attempted to estimate the uncertainties in some of the parameters by varying the values from those of our "best" set given in Tables I and II (designated set 0) and seeing how much change can be accommodated before there is significant decrease in the agreement between any set of calculated and experimental curves. The parameters chosen for analysis were n_2, m_2, n_{-2}, and m_{-2} since they make significant contributions to three of the experimental curves. The direction of variation was defined by a four-dimensional vector connecting the set 0 values with another set which was produced by a least-squares fit to the τ_2^{-1} versus [urea] curve. Changing n_2, m_2, n_{-2}, and m_{-2} by +12%, +18%, −8%, and −6%, respectively, caused a slight improvement in the quality of the fit of the $1/\tau_2$ vs [urea] curve as measured by the chi-square value, although the improvement was difficult to see by visual inspection. These changes, however, also caused a significant decrease in the quality of the fit to the ΔA^{02} vs [urea] curve, both by the chi-square value and visual inspection. Although this example covers only a limited region of parameter space, we feel that the uncertainty in most of the parameters is no more than 20% and is less than that for many of them. A more extensive discussion of the precision of the parameters with additional examples is presented by Pryse (1988).

As an additional test, we have applied this model to kinetic data published previously from another laboratory obtained by a different technique (Tsong, 1977). In that work, the temperature-jump method was used to follow heme absorption relaxations of cytochrome c in 9.0 M urea as a function of pH. The relaxation times and amplitudes of one process, taken from

Table III: Comparison of pH Effects on Different Mechanisms[a]

mechanism	expression for $1/\tau_1$	pH effects
N ⇌ I ⇌ U + H; I + H ⇌ UH	$k'_1 + k'_{-1}\frac{1/K_3 + [U]}{1/K_3 + [U] + [H]}$	[H] shifts equilibrium to U, decreases rate
H + N ⇌ I ⇌ U; N + H ⇌ NH	$k'_1 + k'_{-1}$	no pH dependence on rate
NH ⇌ I ⇌ U; N + H ⇌ NH	same as above	no pH dependence on rate
N ⇌ I + H ⇌ IH; I ⇌ U	$k'_{-1} + k'_1\frac{1/K_3 + [I]}{1/K_3 + [H] + [I]}$	[H] has no effect on equilibrium
N ⇌ IH ⇌ I + H; I ⇌ U	same as above	[H] shifts equilibrium to N
N ⇌ I + H ⇌ IH; IH ⇌ U	$k'_{-1} + k'_1\frac{[H] + [U]}{1/K_3 + [H] + [I]}$	[H] increases rate
N ⇌ IH ⇌ U; I + H ⇌ IH	same as above	[H] increases rate
N ⇌ I ⇌ UH; U + H ⇌ UH	$k'_1 + k'_{-1}\frac{[H] + [U]}{1/K_3 + [H] + [U]}$	[H] increases rate

[a] k'_1 and k'_{-1} are the rate constants for the I ⇌ U reaction in the three-step mechanism. K_3 is the equilibrium constant for the protonation reaction.

Tsong's Figure 3, are shown in Figure 8. The inverse relaxation time, τ_2^{-1} in Tsong's notation, increases with pH. The amplitude of the Soret absorbance change reaches a maximum around pH 5 and changes sign about pH 6. This complex dependence of the amplitude, particularly the change of sign, provides a stringent test for any proposed model. Our kinetic data make it clear that this process is the same as our I ⇌ U reaction. For example, our τ_1 values at pH 6 and pH 3 in high urea are 4 ms and 15 ms (Bruckman, 1977), while Tsong's are 3 ms and 14 ms.

The simplest extension of our two-step model which would take pH effects into account is a protonation of one of the three species. The three steps can be arranged in eight different ways, as shown in Table III. If the protonation is assumed to be very much faster than the other two reactions, there are only six different expressions for the relaxation time of interest, however. The rate is independent of pH in two of these, and it decreases with pH in two. Of the two expressions that correctly predict the increase of τ_1^{-1} with pH, one predicts that acid stabilizes the native form. Thus, all mechanisms except one can be excluded on qualitative grounds. This mechanism was examined further to see if it is quantitatively consistent with the rate and amplitude data.

The expression for the rate is

$$\tau_1^{-1} = k'_1 + k'_{-1}\left[1 + \frac{K_3P}{1 + 1/K'_1 + K_3[H]}\right] \times \left[1 + K_3\left([H] + \frac{P}{1 + 1/K'_1 + K_3[H]}\right)\right]^{-1} \quad (12)$$

where P = total protein concentration and [H] = hydrogen ion concentration.

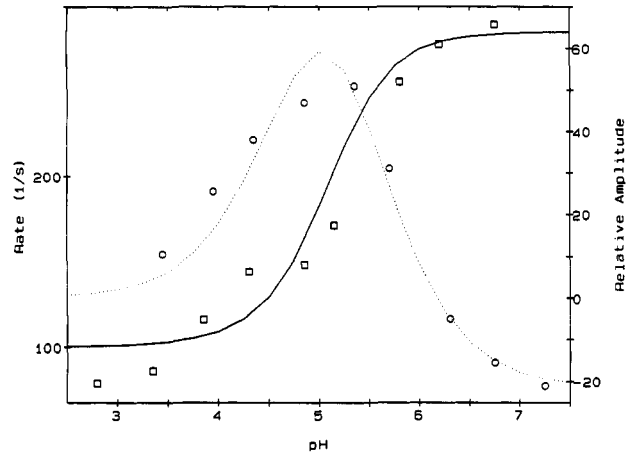

FIGURE 8: Kinetic data from Tsong (1977). Temperature-jump experiments in 9.0 M urea monitoring absorbance at 395 nm: □, $1/\tau$; ○, relative kinetic amplitudes. Solid and dotted lines are calculated from the extended model described in the text.

The amplitude is proportional to the concentration change of species I:

$$\Delta C_I^{01} = -P\frac{K'_1(1 + K_3[H])}{(1 + K'_1(1 + K_3[H]))}\left[\frac{\Delta K'_1}{K'_1} + \frac{\Delta K_3}{K_3}\left\{\frac{K_3[H]}{1 + K_3[H]}\right\}\right] \quad (13)$$

The first factor in eq 13, involving only K'_1 and K_3, varies in magnitude as [H] varies but is always positive. The second factor, however, can change sign if (1) $\Delta K'_1/K'_1$ and $\Delta K_3/K_3$ are of opposite sign (i.e., the enthalpy changes $\Delta H'_1$ and ΔH_3 are of opposite sign) and (2) $\Delta K_3/K_3$ is larger in magnitude

than $\Delta K'_1/K'_1$. When these conditions are met, the full expression for the amplitude varies in magnitude and changes sign as the pH changes. We have used the following values in eqs 12 and 13 to calculate the curves shown in Figure 8: $k'_1 = 100\ s^{-1}$, $k'_{-1} = 260\ s^{-1}$, $K_3 = 4.3 \times 10^5\ M^{-1}$, and $\Delta H_3/\Delta H'_1 = -4.4$. The agreement with the experiment data is quite good.

There is an apparent inconsistency between these numbers and those given in Table I. The equilibrium constant $K_1 = [U]/[I] \approx 3$ in the two-step model should be the same numerically as the apparent equilibrium constant $K_1(1 + K_3[H]) = ([U] + [UH])/[I] \approx 17$ in the three-step protonation model. Attempts to reconcile these values resulted in significantly poorer agreement with either our data or that of Tsong. The reason for the difference probably lies in the different experimental conditions. The temperature-jump experiments were conducted in 0.10 M NaCl, while the pressure perturbation data presented in this paper were obtained under low-salt conditions. We have also conducted RPPK experiments at varying NaCl concentrations. Analysis of the pressure perturbation data at 0.10 M NaCl gave $K_1 \approx 16$ at 9 M urea (Pryse, 1988).

From the ratio $\Delta H_3/\Delta H'_1$ given above, we can calculate the value of $\Delta H'_1$ to be $\approx$1.6 kcal/mol, assuming that the enthalpy change for the protonation of His-18 under these conditions is the same as that of the amino acid in aqueous solution, which is −6.9 kcal/mol. The value of K_3 given above, $4.3 \times 10^5\ M^{-1}$, is less than the normal value for histidine in water, $\approx 10^6\ M^{-1}$, due in part to the large positive charge on the protein at pH 4.0.

Discussion

A major difficulty in studies of protein folding kinetics is relating the measured, typically spectroscopic, parameters to protein conformational changes and to specific structural events. Our RPPK measurements have used three different spectroscopic probes to monitor the reaction progress. Each of these probes is sensitive to a different aspect of the protein's structure. Soret absorbance mainly reports changes in the spin state of the heme iron due to changes in its two axial ligands. The 695-nm band is sensitive to the presence of the Met-80 ligand, but not at all to the His-18 ligand. Trp-59 fluorescence depends on the distance of the residue from the heme and is highly correlated with the overall dimensions of the polypeptide chain (Tsong, 1974).

In the folded conformation the axial ligands are His-18 and Met-80. Their detachment from the heme is coupled to larger conformational changes. We must first determine how the axial ligands contribute to the measurements and then characterize the larger associated protein conformational changes.

Our measurements show that the fast and slow processes correspond to the attachment of His-18 and Met-80, respectively, as axial ligands. This assignment is based on the following equilibrium and kinetic data. (1) The 695-nm band indicates the presence of the methionine–iron bond (Sreenathan & Taylor, 1971; Folin et al., 1972). Under conditions in which both processes are observed in the Soret band, only the slower step is seen when the 695-nm band is monitored. (2) The equilibrium absorbance change at 695 nm coincides with the amplitude of the slow kinetic process. (3) The fast process occurs at high urea concentrations at which the 695-nm band is no longer present. Since RPPK measurements are initiated by a perturbation of the reaction equilibrium and since Met-80 has been detached from the heme at high urea concentrations, the fast step cannot involve the displacement of Met-80 from the heme. (4) The fast process is observed in the cyanogen bromide fragment (residues 1–64) which contains neither Met-80 nor Met-65. (5) The pH dependence of the fast process is consistent with protonation of a histidine residue.

A study using hydrogen exchange, rapid mixing, and NMR techniques in combination provides complementary structural information on the folding of cytochrome *c* in guanidine hydrochloride (Roder et al., 1988). They found that within 10 ms several amide protons in the N- and C-terminal helices gain protection against hydrogen exchange, and Trp-59 is significantly quenched. Other parts of the protein gain protection on a 400-ms time scale. They suggest that the terminal helices form and possibly dock to a native-like conformation during the fast step. The similarity of the kinetics indicates that the initial folding step, and hence the folding intermediate, might be the same under the two sets of conditions. If this is true, then at least three specific structural events are occurring during the initial folding step: formation of the terminal helices, ligation of His-18, and movement of Trp-59 closer to the heme. This would also mean that there is a significant amount of helix present at urea concentrations higher than 5 M, since we have shown that the intermediate form is about 25–35% of the total protein in concentrated urea. This is an interesting possibility which merits further experimental testing, especially since a recent paper has shown that native-like helical segments exist with surprising stability under conditions (pD 2.2, 0.02 M NaCl, 20 °C) where the protein is in an extended, noncompact form with few tertiary structural hydrogen bonds (Jeng & Englander, 1991).

Viscosity and Trp-59 fluorescence provide more general measures of conformational change. From our values of K_1 and K_2 and earlier data on the fluorescence and viscosity under various conditions, we can estimate the viscosity to be $\approx$15 mL/g for the I form and >23 mL/g for the U form (Tsong, 1975, 1976; Babul & Stellwagen, 1972; Bruckman, 1977). These values are consistent with a random coil and an extended chain, respectively.

The intermediate form is probably not a random coil, however, on the basis of the structural interpretation presented above and also of the expectation that the transition from an extended linear chain to a random coil should be much faster than the observed 10 ms. Indeed, the simplest structural interpretation of the fast reaction would take account of the fact that there are only 6 rotatable bonds connecting His-18 to the heme. A Brownian dynamics simulation of a 24-residue polypeptide suggests that a simple association of His-18 with the heme iron, limited only by the rotations of the bonds between the histidine and the heme, should occur in the time range of nanoseconds (Lee et al., 1987). The 10-ms relaxation time of the I to U transition indicates that other processes must also be taking place.

The extent of the conformational change in each step can also be estimated from the solvent dependence of the equilibrium constants. In multiple binding theory, the transition sharpness is related to the difference in the number of equivalent, independent binding sites on each form. In a more general thermodynamic formulation, $\partial \ln K/\partial[\text{urea}]$ is related to the difference in virial coefficients for the interaction of urea with the two protein forms (Schellman, 1978). When several simplifying assumptions are made, the transition sharpness is proportional to the change in surface area. Both of these approaches support the conclusions that the intermediate form is almost as solvent-exposed as the unfolded form and that most of the compact structure is formed during the I $\rightleftharpoons$ N step.

These theories can also be applied to the solvent dependence of the rate constants. The unfolding rate constant is influenced

by the difference in the number of binding sites (or in the surface area) between the native and the transition states, and the folding rate constant is influenced by the difference between the transition and the denatured states. The changes in the folding and unfolding rate constants with urea concentration are roughly equal in magnitude for step 2 (Table I). This implies that the transition state is approximately midway between the N and I conformations in terms of denaturant binding sites or solvent-accessible surface area.

The volume changes of the two steps are approximately equal, about −15 mL/mol. There is no simple relation between the size of the volume change and the magnitude of the conformational change, because the volume change for protein folding is the sum of positive and negative partial volume changes. A discussion of the volume changes is therefore deferred to a later paper where pH and ionic strength effects are examined.

Relationship to Other Studies. The two reactions which we observe by pressure perturbation have been seen by other workers under different conditions, although they have been interpreted in different ways. We have shown above that our extended model is consistent with Tsong's data on the 10-ms step, which was originally attributed to the binding of hydroxide ion to the heme iron (Tsong, 1977). A more extensive analysis shows that this proposal is probably not correct (Pryse, 1988).

The slow step has been seen at denaturing pH's (pH 1.0–3.0) in the absence of chemical denaturants using both temperature jump and stopped flow (Dyson & Beattie, 1982). A 200-μs relaxation, which is too fast to be seen with the RPPK technique, was also observed using temperature jump, but a 10-ms step was not observed with either T-jump or stopped flow. These experimental results are not inconsistent with ours. If the 200-μs step has a volume change of zero, it would not appear even as a rapid absorbance change during the rise time of the pressure change, but it would change with the same rate as the slower unfolding process to which it is coupled. If the 10-ms step which we see has an enthalpy change of zero under their conditions, then the T-jump measurements would not perturb this mode.

Dyson and Beattie proposed a mechanism in which a protonation triggers detachment of Met-80 and changes the heme iron from low spin to high spin without unfolding the polypeptide chain during the 200-μs step. This is followed during the 100-ms step by protonation and detachment of His-18 and a large change in the conformation of the polypeptide chain. Tsong (1977) had also seen the 200-μs reaction under different conditions and interpreted it as detachment of His-18. In contrast to these proposals, the results described here, particularly the kinetic experiments monitoring the 695-nm band, show clearly that Met-80 detaches in the 100-ms step and His-18 detaches in the 10-ms step. Our results are in agreement with their interpretation that the major conformational change takes place in the slower step.

The kinetics of folding of cytochrome c from yeast is very similar to that from horse (Nall & Landers, 1981; Nall, 1983).

Spectra. The only protein form whose spectrum can be observed directly is the fully native form. Within and beyond the unfolding transition at least two of the protein forms I, U, or N are present. The spectra which we have calculated for the I and U forms are consistent with earlier experimental work on the spectra of cytochrome c and model heme compounds which provide information on the shape and relative positions of the absorption bands and the effect of solvent on the intensity of the absorption (Williams, 1971; Drew & Dickerson, 1978; Nanzyo & Sano, 1968; Harbury & Loach, 1959). These studies show that although the high-spin or low-spin Soret bands of various species may have rather different maxima, the *difference* in wavelength between the high-spin and low-spin bands is about the same, 14–15 nm. Also, the position of the absorption band of the mixed-spin species seems to be restricted to the middle one-third of the range between the other two peaks, that is, 4–10 nm above the high-spin peak. The solvent-dependent increase in ϵ_U which was used in fitting some of the data is also consistent with earlier work (Stellwagen, 1968; Tsong, 1975).

The calculated spectra reproduce the experimental measurements well except at the edges of the absorption bands. On the low-wavelength side, this is due to the presence of a small peak at 360 nm which is not included in the calculations. On the high-wavelength side, the difference exists because we include only a single, "cold" ground state, rather than "thermalizing" the spectra with different ground-state energies. As discussed by Champion and Albrecht (1979), the primary effect of using a single ground state is to decrease the red edge intensity. Neither of these contributions should affect the calculated kinetic amplitudes.

The spectra shown in Figure 1 contradict an assumption sometimes made in equilibrium and kinetic models. The extinction coefficient of the intermediate form is not always intermediate to those of the native and unfolded forms. For some wavelengths this is true, but there is a range for which the extinction coefficient of the intermediate is larger than that of either the native or unfolded forms. The repetitive pressure perturbation technique can measure kinetic amplitudes rapidly at many wavelengths using the same small sample, providing information about the kinetic intermediates and reaction mechanism which is not available from data taken at a single wavelength.

Summary. This study demonstrates a unique application of the repetitive pressure perturbation method to the mechanism of protein folding. We have proposed a mechanism for folding and tested it extensively with a global modeling procedure that includes both kinetic and equilibrium data, as well as previously published data from another laboratory. Taken together with earlier results our equilibrium and kinetic measurements support a detailed picture of the structural changes that occur in the two observed folding steps. In the first step, the N- and C-terminal helices form and probably dock, the His-18 axial ligand attaches to the heme, and Trp-59 moves closer to the heme. The chain becomes more compact during this step, indicated by the fairly large decrease in the reduced viscosity, but there is only a small reduction of the solvent-accessible surface area. In the second step, Met-80 attaches to the heme, many intramolecular hydrogen bonds are formed, Trp-59 fluorescence is quenched almost completely, and the chain becomes very compact. There is no evidence for a collapse to a compact, disordered state [cf. Dill (1985)]. Additional studies using this method should provide information on the relative importance of different interactions in determining protein structure and volume changes (Kauzmann, 1987).

Acknowledgments

We thank Bill McConnaughey for his expert technical assistance in setting up and maintaining the repetitive pressure perturbation apparatus.

References

Babul, J., & Stellwagen, E. (1972) *Biochemistry 11*, 1195.
Baldwin, R. L. (1986) *Proc. Natl. Acad. Sci. U.S.A. 83*, 8069.

Bevington, P. R. (1969) *Data Reduction and Error Analysis for the Physical Sciences*, McGraw-Hill, New York.
Brandts, J. F., Oliveira, R. J., & Westort, C. (1970) *Biochemistry 9*, 1038.
Bruckman, T. G. (1977) Ph.D. Thesis, Cornell University, Ithaca, NY.
Clegg, R. M., & Maxfield, B. W. (1976) *Rev. Sci. Instrum. 47*, 1383.
Clegg, R. M., Elson, E. L., & Maxfield, B. W. (1975) *Biopolymers 14*, 883.
Champion, P. M., & Albrecht, A. C. (1979) *J. Chem. Phys. 71*, 1110.
Dill, K. A. (1985) *Biochemistry 24*, 1501.
Drew, H. E., & Dickerson, R. E. (1978) *J. Biol. Chem. 253*, 8420.
Dyson, H. J., & Beattie, J. K. (1982) *J. Biol. Chem. 257*, 2267.
Edsall, J. T., & McKenzie, H. A. (1983) *Adv. Biophys. 16*, 53.
Eigen, M., & de Maeyer, L. (1963) *Technique of Organic Chemistry* (Friess, S. L., Lewis, E. S., & Weissberger, A., Eds.) Vol. VIII, Part 2, p 895, Wiley-Interscience, New York.
Folin, M., Azzi, A., & Tamburro, A. M. (1972) *Biochem. Biophys. Acta 285*, 337.
Halvorson, H. R. (1979) *Biochemistry 18*, 2480.
Harbury, H. A., & Loach, P. A. (1959) *Proc. Natl. Acad. Sci. U.S.A. 45*, 1344.
Ikai, A., Fish, W. W., & Tanford, C. (1973) *J. Mol. Biol. 73*, 165.
Jeng, M.-F., & Englander, S. W. (1991) *J. Mol. Biol. 221*, 1045.
Kauzmann, W. (1959) *Adv. Protein Chem. 14*, 1.
Kauzmann, W. (1987) *Nature (London) 325*, 763.
Lee, S., Karplus, M., Bashford, D., & Weaver, D. (1987) *Biopolymers 26*, 481.
Macgregor, R. B., & Clegg, R. M. (1987) *Biopolymers 26*, 2103.
Macgregor, R. B., Clegg, R. M., & Jovin, T. M. (1985) *Biochemistry 24*, 5503.
Myer, Y. P. (1980) *Biochemistry 19*, 199.
Nall, B. T. (1983) *Biochemistry 22*, 1423.
Nall, B. T., & Landers, T. A. (1981) *Biochemistry 20*, 5403.
Nanzyo, N., & Sano, S. (1968) *J. Biol. Chem. 243*, 3431.
Privalov, P. L. (1979) *Adv. Protein Chem. 33*, 167.
Privalov, P. L., & Gill, S. J. (1988) *Adv. Protein Chem. 39*, 191.
Pryse, K. M. (1988) Ph.D. Thesis, Cornell University, Ithaca, NY.
Roder, H., Elöve, G. A., & Englander, S. W. (1991) *Nature (London) 335*, 700.
Schellman, J. A. (1978) *Biopolymers 17*, 1305.
Sreenathan, B. R., & Taylor, C. P. S. (1971) *Biochem. Biophys. Res. Commun. 42*, 1122.
Stellwagen, E. (1968) *Biochemistry 7*, 2496.
Tsong, T. Y. (1974) *J. Biol. Chem. 249*, 1988.
Tsong, T. Y. (1975) *Biochemistry 14*, 1542.
Tsong, T. Y. (1976) *Biochemistry 15*, 5467.
Tsong, T. Y. (1977) *J. Biol. Chem. 252*, 8778.
Williams, R. J. P. (1971) *Cold Spring Harbor Symp. Quant. Biol. 36*, 53.

Determination of the Molecular Dynamics of Alamethicin Using ^{13}C NMR: Implications for the Mechanism of Gating of a Voltage-Dependent Channel†

Laurie P. Kelsh, Jeffrey F. Ellena, and David S. Cafiso*
Department of Chemistry and Biophysics Program, University of Virginia, Charlottesville, Virginia 22901
Received August 2, 1991; Revised Manuscript Received December 30, 1991

ABSTRACT: Alamethicin is a channel-forming peptide antibiotic that produces a highly voltage-dependent conductance in planar bilayers. To provide insight into the mechanisms for its voltage dependence, the dynamics of the peptide were examined in solution using nuclear magnetic resonance. Natural-abundance ^{13}C spin–lattice relaxation rates and ^{13}C–^{1}H nuclear Overhauser effects of alamethicin were measured at two magnetic field strengths in methanol. This information was interpreted using a model-free approach to obtain values for the overall correlation times as well as the rates and amplitudes of the internal motions of the peptide. The picosecond, internal motions of alamethicin are highly restricted along the peptide backbone and indicate that it behaves as a rigid helical rod in solution. The side chain carbons exhibit increased segmental motion as their distance from the peptide backbone is increased; however, these motions are not unrestricted. Methyl group dynamics are also consistent with the restricted motions observed for the backbone carbons. There is no evidence from these dynamics measurements for a hinged motion of the peptide about proline-14. Alamethicin appears to be slightly less structured in methanol than in the membrane; as a result, alamethicin is also expected to behave as a rigid helix in the membrane. This suggests that the gating of this peptide involves changes in the orientation of the entire helix, rather than the movement of a segment of the peptide backbone.

Voltage-dependent conformational transitions in membrane proteins are of central importance to many processes such as information transfer in the nervous system and energy transduction. As a result, the elucidation of these mechanisms even in simple model systems has been actively pursued. Alamethicin is a small, 20 amino acid peptide that produces a dramatic voltage-dependent conductance when incorporated into planar bilayers or lipid vesicles. This voltage dependence and alamethicin's tractable size have made it an attractive

† This work was supported by a grant from the National Institutes of Health (GM-35215 to D.S.C.).

0006-2960/92/0431-5136$03.00/0